This paper prepared for poster presentation at:
HydroVision International 2013
July 23-26, 2013 -- Denver, CO

NEW TESTING OF COANDA-EFFECT SCREEN CAPACITIES

Tony L. Wahl[1]

ABSTRACT

Coanda-effect screens offer an economical means for removing debris at small hydropower intakes. The screens remove debris from a supercritical flow that passes over a wedge wire screen panel installed with wires oriented horizontally, perpendicular to the flow direction. Individual wires are tilted so that the leading edge of each wire projects into the flow, causing the screen to shear a thin layer of the flow from the bottom of the water column at each slot opening. The screens are largely self-cleaning, with a high flow capacity and minimal need for routine maintenance. This makes them especially useful for remote sites. Capacity of Coanda-effect screens has been related in the past to basic hydraulic parameters, such as the Froude, Reynolds, and Weber numbers of the flow over the screen. New testing over a broader range of flow conditions has led to a better understanding of the variables affecting screen performance, and a new model for predicting the screen discharge coefficient has been developed in which the angle of attack of the flow to the screen slot opening is the crucial parameter. The new model predicts significantly higher flow capacities for typical small-hydro intake configurations.

Keywords: screens, Coanda effect, hydraulic modeling, discharge coefficients

INTRODUCTION

Coanda-effect screens provide high-capacity separation of fine debris from flowing water at agricultural diversions and small hydropower intakes like that shown in Figure 1. The screens operate by removing clean water from a debris-laden supercritical flow that passes over a wedge wire screen panel whose wires are oriented horizontally, perpendicular to the flow direction. The individual wires are tilted along their axes so that the leading edge of each wire projects into the flow, causing the screen to shear a thin layer of the flow from the bottom of the water column at each slot opening. The screens have been marketed for many years by several companies using the name *Coanda-effect screen* because the Coanda effect causes flow to remain attached to the top surface of each wire, thus enhancing the shearing action. The primary variables describing a Coanda-effect screen are shown in Figure 2.

The Bureau of Reclamation performed research (Wahl 2001) to develop methods for computing the hydraulic capacity of Coanda-effect screens. That work related screen capacity to the Froude, Reynolds, and Weber numbers of the flow over the screen. Recent investigations showed that this method for predicting screen capacity was inaccurate when extended to flow conditions outside of the range of previous tests (higher velocities and Reynolds numbers). This paper describes a new laboratory facility that was recently constructed to test a variety of Coanda-effect screen materials over a wide range of flow conditions. Testing results and improved methods for predicting screen capacity are described.

[1] Hydraulic Engineer, Bureau of Reclamation Hydraulics Laboratory, Denver, CO, USA. 303-445-2155, twahl@usbr.gov.

Figure 1. — Typical Coanda-effect screen intake for a small hydropower development.

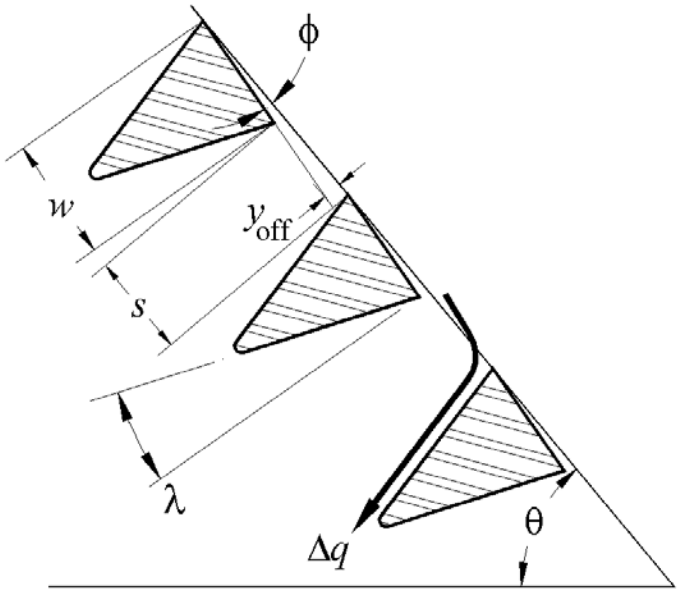

Figure 2. — Close-up edge view of a Coanda-effect screen illustrating wire parameters.

EXPERIMENTAL SETUP

A small-scale facility was constructed in the hydraulics laboratory to determine screen throughput under a range of hydraulic conditions. The facility is similar conceptually to that

used for studies reported in Wahl (2001), but with greater flexibility to perform testing over a broad range of flow conditions. Figure 3 shows components of the test facility, including the head tank, a 6-inch (0.15-m) wide adjustable-slope flume with three available screen test locations (top, middle, bottom), two V-notch weirs for measurement of screened flows, and a tailwater tank. Flow rates up to 0.26 ft^3/s (442 L/min) can be provided into the head tank. Water flows out of the head tank, down the sloped flume, and across the screen being tested. Some flow passes through the screen; flow through the most upstream slots is collected and measured, but is considered wasted, while the flow through the downstream slots is also collected and measured and comprises the primary test result. All tests described in this paper were carried out with the flume at a 15° slope, with the exception of one series of validation tests performed at a 30° slope. At the 15° slope, velocities at the screen test positions varied from 5.25 to 8.2 ft/s (1.6 to 2.5 m/s), and depths ranged up to about 0.94 in. (2.4 cm). Froude numbers at the top of the screens ranged from about 3.8 to 10. Froude numbers in this study were computed from $\mathrm{Fr} = V / \sqrt{gD\cos\theta}$ where Fr is the Froude number, V is the flow velocity, g is the acceleration due to gravity, D is the hydraulic depth, and θ is the slope of the screen panel.

Figure 4 and Figure 5 show close-up views of the screen test locations and the special flow collector box used to capture the flow that passes through the screen. The collector box is divided into upstream and downstream compartments so that the flow through the first half of the screen can be collected and measured separately from the flow through the second half of the screen. This allows proper development of the flow profile above the screen face before the flow reaches the test section (the downstream half of the screen). Because flow approaching the first half of the screen has not had an opportunity to align with the face of the tilted wires (it is initially aligned with the flume slope), the flow rate through the first few wire slots is lower than the flow through the downstream slots. This configuration allows the test section to accurately represent the performance of a slot located in the midst of an operating screen structure. An adjustable knife-edge divider attached to the bottom of the screen mounting plate (Figure 6) can be positioned exactly at a desired wire position so that the number of waste slots and test slots is known. The collector box is constructed from clear acrylic which permits visual verification that the divider plate is effectively separating the waste flow and tested flow streams.

TESTED SCREENS

Flow test data for six different screen materials are presented in this paper. Table 1 presents the measured dimensions of each tested screen. The A- and B-series screens were very similar to one another, with nominal 2 mm slots and 3/16-inch wires. The only significant differences between them were the wire relief angle and the fact that the B-series screens had a machined-sharp leading edge on the profile wires, whereas the A-series screens were manufactured with a slightly rounded edge estimated to have an edge radius of 0.005 in. The #1 and #3 screens were previously tested by Wahl (2001) and were re-tested in the new laboratory facility. They also had a slightly rounded leading edge, with an unknown edge radius. Wire tilt angles for all screens were measured with the optical light reflection technique described in Wahl (2001). The wire tilt angles shown are the average of multiple (2 or 3) sets of measurements carried out on separate days to ensure repeatability. Each set of measurements evaluated the tilt of each individual wire in the section of the sample screen that would be tested for flow capacity.

Figure 3. — Screen test facility.

Figure 4. — Close-up views of a screen and the collection box beneath the flume.

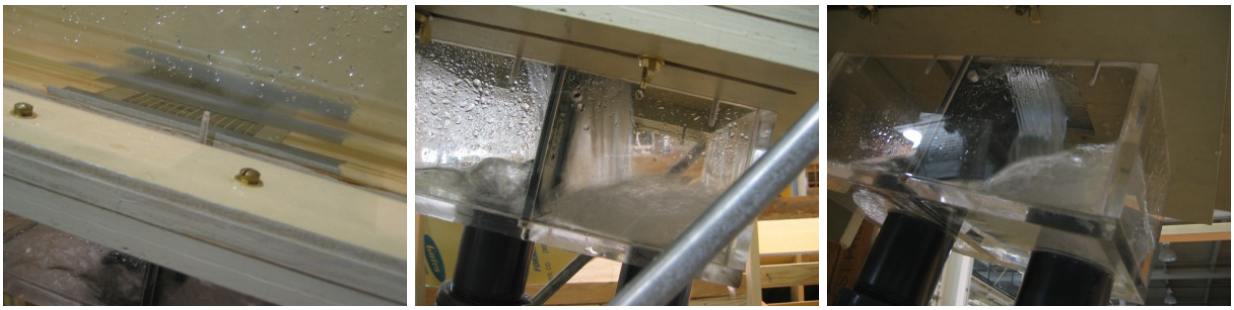

Figure 5. — Flow divider box in operation.

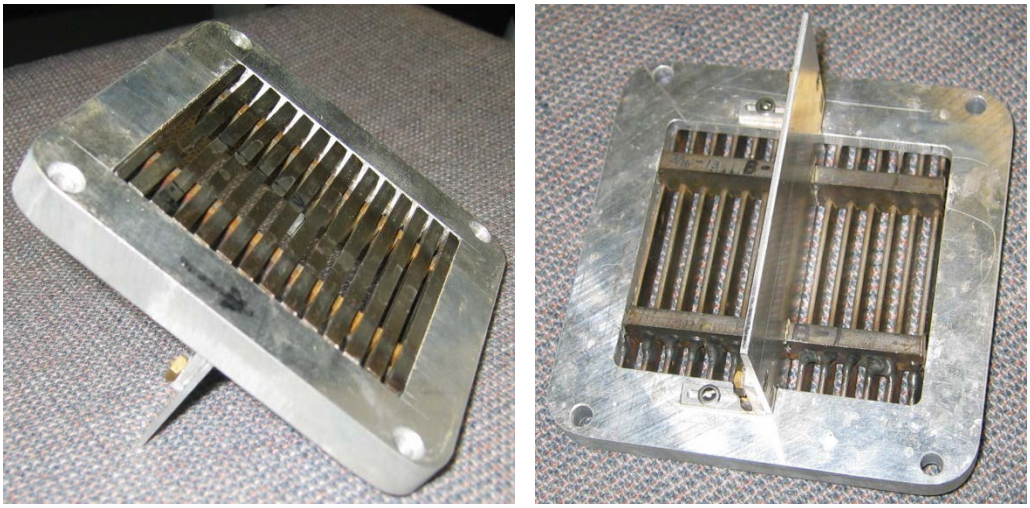

Figure 6. — Test screen B-1 in mounting block and a view of the underside of the screen with divider plate installed. Flow is left to right in both photos.

Table 1. — Properties of tested screens.

Screen	A-5	A-8	B-1	B-2	#1	#3
Relief angle, λ (designated, not measured)	10	10	13	13	17.5	11
TILT ANGLE, degrees	5.6	6.9	4.3	6.5	3.82	6.88
Avg. slot width, s (mm)	1.99	1.96	2.05	2.05	1.02	0.47
Avg. wire thickness, w (mm)	4.72	4.74	4.60	4.62	2.39	1.50
Width, inches	3	3	3.5	3.5	3.66	3.44
Length, inches	3.125	3.125	3.5	3.5	3	2.875
Support bar spacing, inches	2.125	2.125	2	2.0625	2.75	0.53125
Support bars	3/8" round	3/8" round	1/4" square	1/4" square	3/8" round	1/8" square
Notes			sharp wires	sharp wires		

TESTING

Screens were tested at all three positions (top, middle, and bottom) in the flume, which allowed for a range of depths, velocities, and Froude numbers to be produced. The test width of each screen was set by masking off a width equal to an integer multiple of the spacing interval of the underlying support bars. At each location the flow rate into the flume was set to at least three different flow rates spanning the capacity of the supply pump in the facility. Flow rates into the test flume were measured by an acoustic transit time meter installed on the 2" PVC pipe feeding the head tank. Data were also collected over the course of the testing that allowed calibration of the crest of the test flume so that it could serve as the inflow measurement device. Flow rates through the first half of the test screen (the "waste" section) and the second half (the "test" section) were measured using the two V-notch weir tanks. Initially, the flows through the V-notch weirs were computed using a theoretical relation based on the weir geometry, but over the course of the testing, data were also collected to calibrate the weirs in place. These calibrations were developed by making independent volume-and-time measurements of flow through the weir openings using a 4 L graduated cylinder and handheld stopwatch. This led to the development of a unique head-discharge relation for each weir, and these relations were used for the final processing of the test data. The uncertainties of these calibration relations at the 95% confidence level for the inflow and the two screened flows (the V-notch weirs were interchanged between the waste flow and test flow at various times during the testing) were estimated to be ±2.2%, ±6.5%, and ±5.0%, respectively.

The majority of the tests were conducted with the flume at a 15° slope. For validation purposes, one series of tests was made with the flume set on a 30° slope.

RESULTS

Wahl (2001) developed a discharge equation for the flow through each slot of a Coanda-effect screen:

$$\Delta q = C_{cv} C_{\mathrm{Fr}} s' \sqrt{2gE}$$

where Δq is the discharge through the slot per unit width of screen structure, C_{Fr} is a coefficient that is a unique function of the screen geometry and the Froude number of the flow, s' is the slot width measured from the tail of one wire to the leading tip of the next wire, and E is the specific energy of the flow above the screen face (sum of depth and velocity head). The coefficient C_{cv} is a calibration coefficient that is believed to account for the effects of flow contraction through the slots, nonuniform velocity distribution, and other real fluid effects. Based on tests of three screens with varying wire geometry, Wahl (2001) developed a predictive equation that related C_{cv} to the Froude number (Fr), Reynolds number (Re) and Weber number (We) of the flow above the screen (the latter two computed using the slot width as the reference length parameter). These dimensionless flow parameters are, respectively, the ratios of the inertial and gravitational forces, viscous and inertial forces, and surface tension and inertial forces.

The data collected from these tests were initially used to compute values of C_{cv} for each test and compare them to values predicted by Eq. 11 from Wahl (2001) in which $C_{cv}=f$(Fr, Re, We). This

effectively normalizes the test results, accounting for basic differences in screen geometry such as different slot widths and different wire tilt angles. This allows for an evaluation of the accuracy of the Wahl (2001) equation for predicting screen performance. Figure 7 shows the results graphically.

Careful examination of Figure 7 shows that in general the B-series screens accept more flow than the A-series screens (higher observed values of C_{cv}). This could be due to the different wire relief angles, but is more likely a result of the sharpness of the B-series wires. The comparison of observed C_{cv} values to those predicted by the Wahl (2001) equation is poor, both across the range of screens tested, and across the three flume locations (top, middle, bottom) for individual screens. In general, higher values of C_{cv} occur at the lower test positions. For the A-series screens there is reasonable agreement with predicted values at the middle and bottom positions, but observed values of C_{cv} at the top test position are much lower than those predicted by the Wahl (2001) equation. For the B-series screens the observed values of C_{cv} at the lower test positions are much higher than expected. The discharge prediction model developed in Wahl (2001) should fully account for variations of depth, velocity and Froude number at the different test positions, but the model is clearly failing to account for a systematic change in the screen performance as a function of a flow parameter associated with the test location. The Wahl (2001) equation also does not predict a performance difference between the A- and B-series screens (since they have nominally equal wire widths and slot angles), but it is clear that they do have significantly different flow capacities.

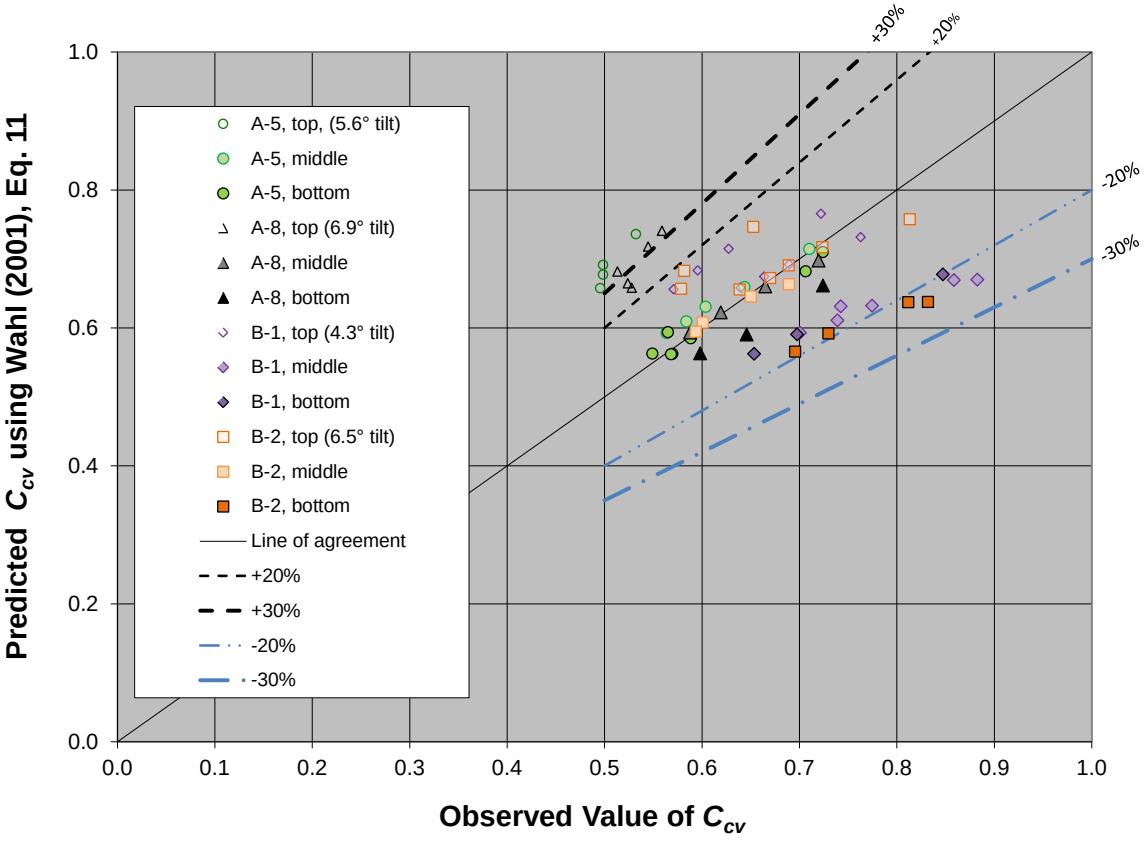

Figure 7. — Screen test results showing observed and predicted C_{cv} values for the A- and B-series screens tested at the three different flume locations.

These observations were noted early in the test program (before all of the data in Figure 7 had been collected), and were at first attributed to experimental error or systematic biases that were not controlled during the testing. Procedures were instituted to zero all water level sensors (point gages in stilling wells) at the beginning of each test run, in-place calibrations of weirs were re-checked, wire tilt angles were re-measured and verified, and some test runs were repeated. While these efforts did marginally improve the quality of the test data, they did not change the systematic performance differences shown in Figure 7.

ANALYSIS

Ultimately, it was determined that a new predictive model for C_{cv} was needed. The data were analyzed further in an attempt to find systematic differences in screen capacity that could be uniquely associated with specific flow parameters or screen geometry. Relations to numerous parameters were explored and the best relation was found to be with the computed angle of attack of the flow to the screen slot opening. This is the angle $\delta+\psi$ shown in Figure 8. The approach flow vector V_r represents the resultant of the velocity across the screen face and the velocity perpendicular to the screen face that would be obtained by converting the pressure head associated with the depth of flow into velocity head.

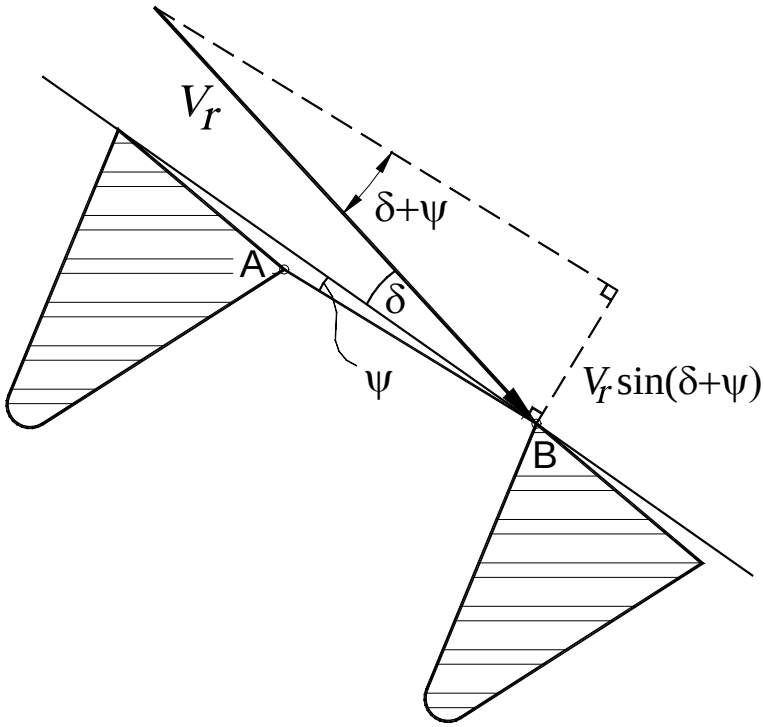

Figure 8. — Idealized flow approaching a single slot opening in a Coanda-effect screen.

Figure 9 shows values of C_{cv} plotted versus the attack angle, $\delta+\psi$, for the A-series and B-series screens, and for screens #1 and #3. The figure includes data collected at all three positions in the flume (top, middle, and bottom), and one data set that was collected with the flume set at a 30° slope for validation purposes. The figure shows that the A- and B-series screens have a similar

form of relation to the attack angle, with a small shift in the shape and location of the best-fit curve through the data. Screen #1 also exhibits a similar type of relation between C_{cv} and the angle of attack. Screen #3 exhibits a somewhat similar trend in C_{cv} versus angle of attack, but with significantly greater scatter in the data. Figure 10 shows a more detailed breakdown of the data for screens #1 and #3, separated by test location and date of testing. The performance of screen #1 is very consistent, while the performance of screen #3 is inconsistent.

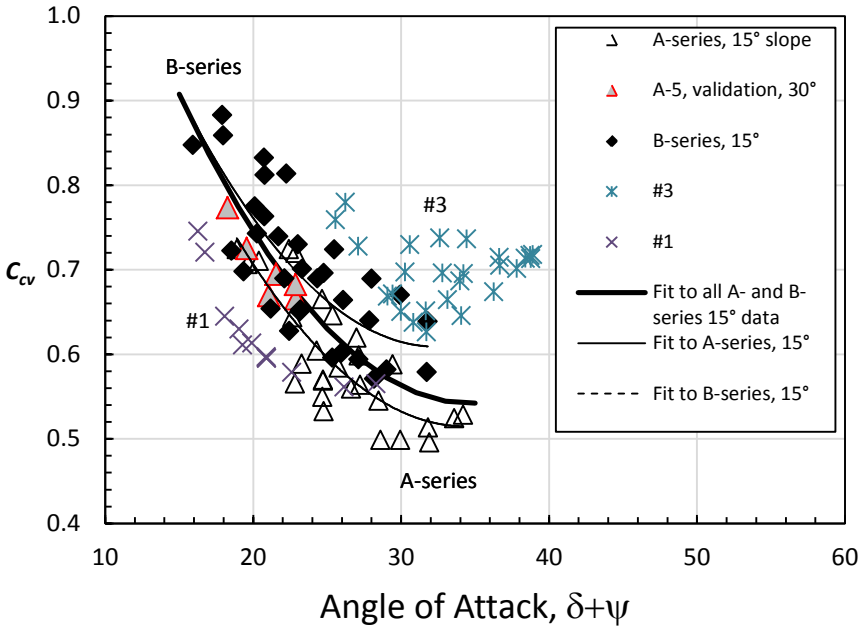

Figure 9. — Relation between C_{cv} and flow attack angle for A- and B-series screens. Best-fit polynomial lines for the A-series, B-series, and full data sets are shown. Curve fit parameters are given in Table 2.

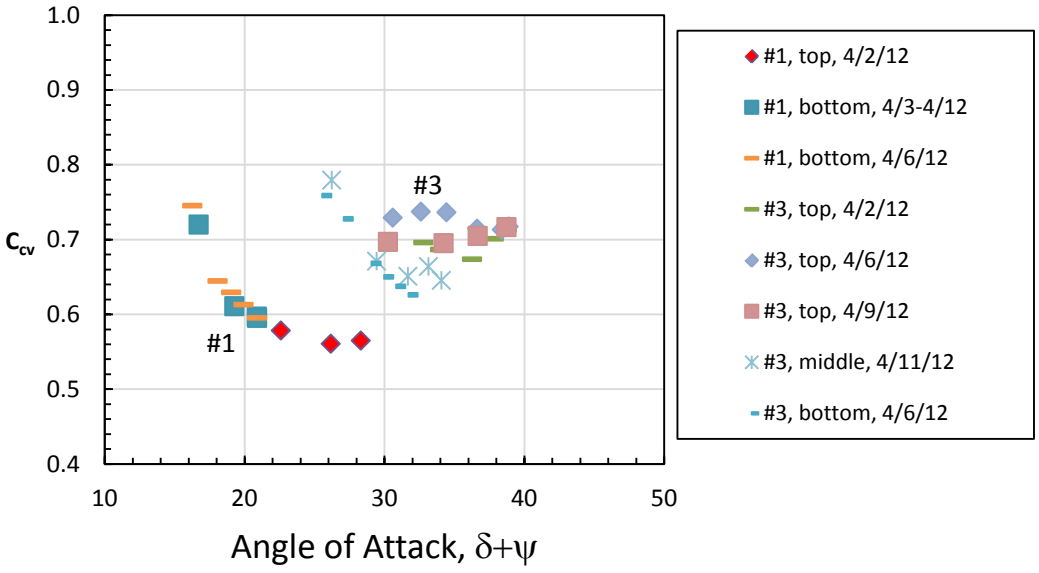

Figure 10. — Detailed view of C_{cv} versus angle of attack data for screens #1 and #3.

Second-order polynomial equations that relate C_{cv} to $\delta+\psi$ were developed for the A- and B-series screens (Table 2). Note that the validation data collected at a 30° slope fits well to the A-series line developed using only the data from the tests at 15° slope. Table 2 includes equation parameters for the A-series screens developed using only the data for 15° slope, and including the validation data collected at 30° slope. Including the 30° data causes only a small change in the curve fit parameters. Specific regression relationships for screens #1 and #3 were not developed, but there is the potential to develop similar relations for them, or for any other screen that is tested in the manner described in this paper.

Table 2. — Parameters of best-fit lines for predicting C_{cv}. Shaded rows are the parameters for the curves shown in Figure 9. The lowest Froude numbers were obtained from tests at the maximum flow capacity of the test facility. The highest Froude numbers were obtained at low flow rates that barely maintained a wetted condition on the last slot of the test screens.

Parameters of $C_{cv}=m_2(\delta+\psi)^2+m_1(\delta+\psi)+b$				Range of supporting data		
Screens	m_2	m_1	b	$\delta+\psi$	**Fr**	V, m/s
A-5 and A-8	0.000933	-0.0641	1.615	19° – 34°	12.8 – 4.0	1.6 – 2.54
B-1 and B-2	0.000990	-0.0641	1.648	16° – 32°	12.3 – 4.1	1.56 – 2.55
A-5, A-8, B-1 and B-2	0.000945	-0.0655	1.678	16° – 34°	12.8 – 4.0	1.56 – 2.55
Validation data set, A-5 on 30° slope, bottom position				18° – 23°	14.2 – 7.8	2.34 – 2.69
A-5 and A-8, including validation data	0.000965	-0.0665	1.657	18° – 34°	14.2 – 4.0	1.6 – 2.69
All data from A- and B-series screens (including validation data)	0.000906	-0.0631	1.642	16° – 34°	14.2 – 4.0	1.56 – 2.69
#1	0.002283	-0.1148	1.995	16° – 28°	10.7 – 4.0	1.63 – 2.53
#3	0.001493	-0.0986	2.301	16° – 34°	13.8 – 4.1	1.57 – 2.53

Figure 11 and Figure 12 show the data for the A- and B-series screens in more detail. Note that at times data collected from different locations seemed to follow a single tight relation to the angle of attack (e.g., A-5, top on 3/23/12 and A-5, bottom on 4/4/12), but on other dates or at other test locations there were offsets observed from one day or one location to the next. This continued on tests run at later dates (after 4/4/12) when daily calibration procedures were enhanced. There was no discernible, repeatable pattern to these variations and it was concluded that they were evidence of experimental noise that could not be fully eliminated from the tests.

DISCUSSION

The regression equations given in Table 2 represent a new approach to modeling the performance of Coanda-effect screens. The advantage of this approach is that it should produce more accurate modeling of flow capacity across a wide range of flow conditions. Figure 7 showed that the Wahl (2001) equation fit the observations for some cases, but also suffered errors up to ±30% for other flow conditions, utilizing the same screen. The new relations allow the full range of flow conditions for a given screen to be fit to a single model, while recognizing that each wire type can exhibit a unique performance curve.

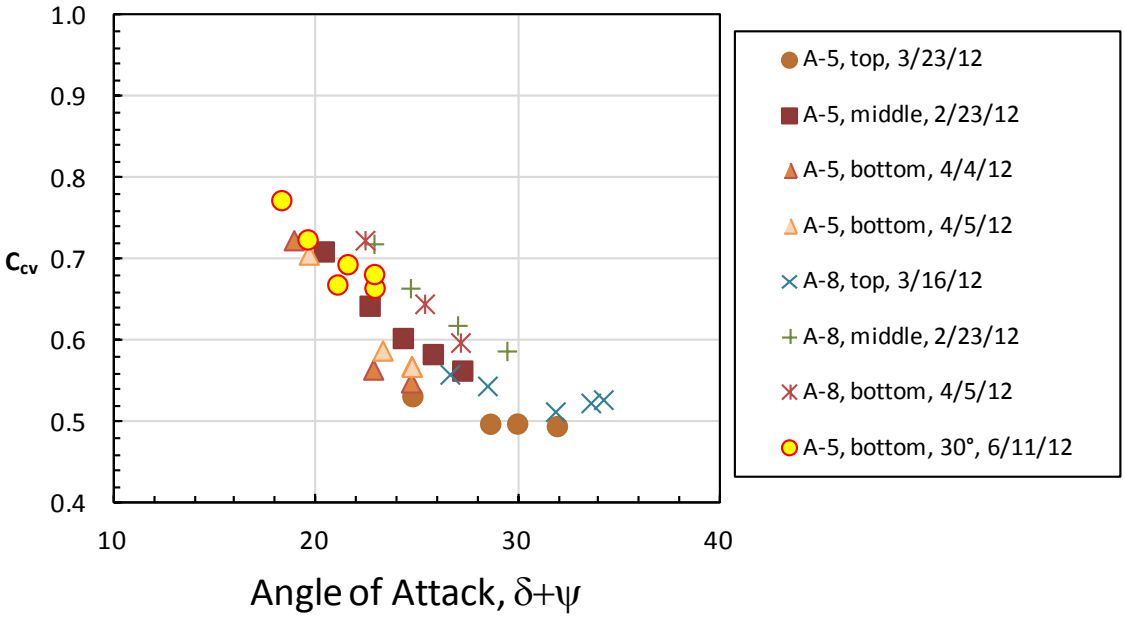

Figure 11. — Test results for screens A-5 and A-8 for different test locations. Legend indicates date on which each test was performed.

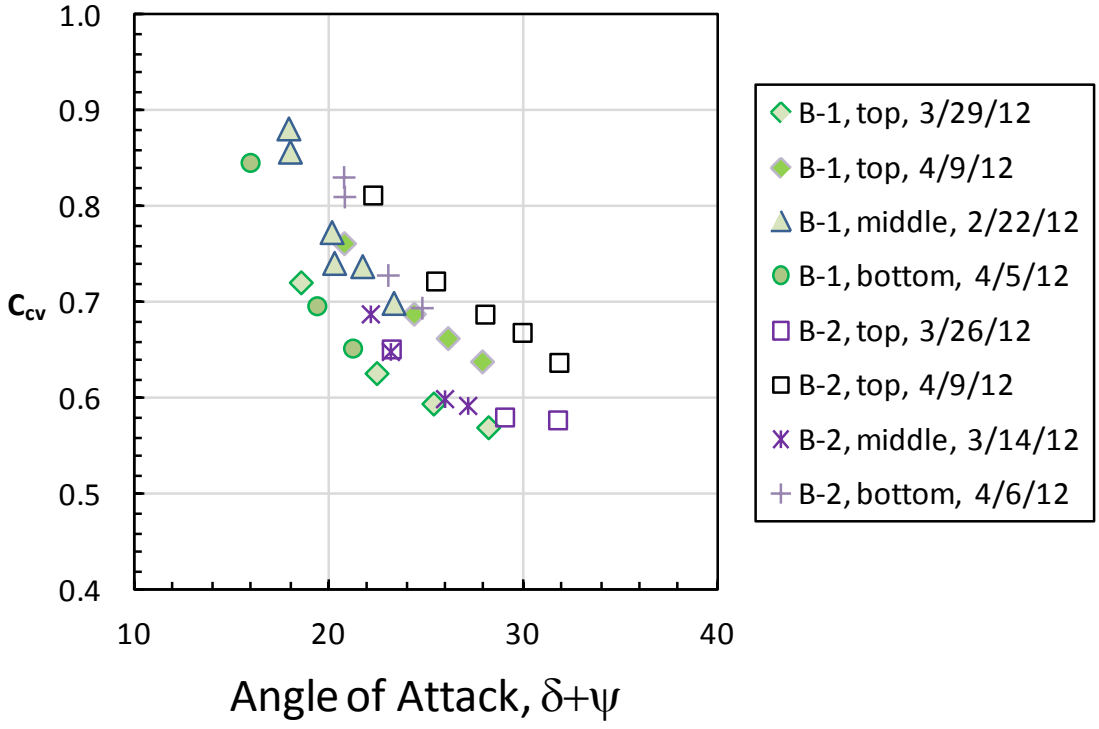

Figure 12. — Test results for screens B-1 and B-2 for different test locations. Legend indicates date on which each test was performed.

To make the equations in Table 2 useful for screen design purposes, they are being incorporated into a new version of the Coanda screen software, version 0.60. This version will provide a default equation for C_{cv} based on testing of a variety of screens and will also offer the user the choice of entering values of m_1, m_2, and b that are unique to a specific screen. Use of the default values would be suggested for untested screens. Parameter values specific to individual screens could be determined by conducting testing like that described in this report. As additional screen configurations are tested, it may be possible to refine the default screen performance model. There is also the possibility that future research could identify factors causing differences in performance for certain screens, which might allow the development of more sophisticated equations.

To assess the impact of the new approach to modeling screen performance, the C_{cv} values determined from the hydraulic tests of the A- and B-series screens were compared to those predicted by the relation developed in Wahl (2001) and the new relations shown in Table 2 (Figure 13). The relations used from Table 2 were those in the second and fifth rows, which were specific to the A-series and B-series screens, utilizing all collected data (including the A-5 validation data at 30° slope).

Figure 13 shows that the new relations more effectively predict the values obtained from the testing. The old equation (Wahl 2001) was

$$C_{cv} = 0.21 + 0.0109(\mathrm{Re}/\mathrm{We}) + 0.00803(\mathrm{Fr})$$

in which C_{cv} was a function of the Froude number, Fr (ratio of inertial to gravitational forces), Reynolds number, Re (ratio of inertial to viscous forces), and Weber number, We (ratio of inertial to surface tension forces). This equation fails to accurately model cases in which the observed values of C_{cv} were either very low or very high. As a result, the standard deviations of the relative errors for the two methods are 16.5% for the old equation and only 7.0% for the new relations. A careful analysis of the old and new equations shows that the source of the errors in the old equation is the dependence on the Reynolds and Weber numbers, the ratio of which is inversely related to the velocity ($\mathrm{Re}/\mathrm{We} \approx \mathrm{V}^{-1}$). Thus, the old equation predicts small C_{cv} values when velocity is high.

The testing by Wahl (2001) covered a different and somewhat smaller range of these dimensionless parameters than the current tests (Re=950 to 4300 and We=29 to 275 for the previous tests versus Re=700 to 5100 and We=16 to 200 for the new tests). The apparent relation to Re and We did not continue when the range of Re and We was extended. Instead, the new tests showed that the screen performance was not sensitive to Re and We, but was instead related to the angle of attack. Wahl (2001) showed that for a single screen the angle of attack is a unique function of the Froude number, so the dependence of the old equation on the Froude number was appropriate. However, the new relations based directly on angle of attack are superior because they incorporate the Froude number and also account for changes in slot spacing, wire thickness and wire tilt angle of specific screens.

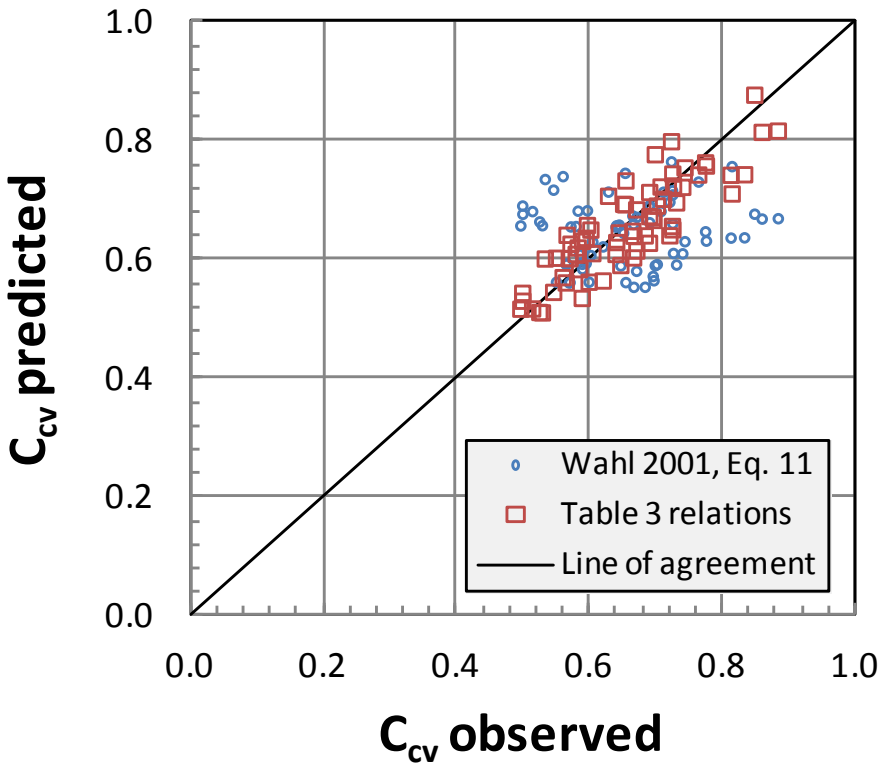

Figure 13. — Predicted C_{cv} values versus observed C_{cv} values.

A practical illustration of the impact of the differences between the old and new methods for predicting C_{cv} is obtained by comparing the flow profiles for a hypothetical specific screen structure. Figure 14 shows flow profiles obtained when C_{cv} values are modeled using the Wahl (2001) equation ("old") and the relations developed in this paper ("new").

Velocity profiles across the screen are almost identical, as expected, but the flow passes through the screen in a much shorter distance using the new equations. At the top of the screen (Distance = 0), the depth and discharge curves obtained with the new equations are nearly tangent to those obtained with the old equations, indicating that the two methods produce similar results. However, as the velocity increases on the lower part of the screen, the old equations predict that the screening efficiency of each slot diminishes, causing the slope of the discharge curve to flatten. Using the new C_{cv} relation, the efficiency of the lower portion of the screen is almost the same as that of the upper part of the screen and the cumulative screened discharge down the length of the screen increases in an almost linear fashion. This result (higher discharge) should be expected for many prototype situations, since it is common for a prototype to require extrapolation of the C_{cv} relation to higher velocity ranges than those tested in the laboratory, but there is usually little need for extrapolation to lower velocity ranges.

FUTURE RESEARCH

This work has shown that a unique relation exists between the C_{cv} coefficient and the flow angle of attack for different screen materials. It is hoped that additional research can be performed on other screens, including screens previously tested by Wahl (2001) and others that are used in

typical Coanda-effect screen installations. The test facility used for this work allows for a wide range of flow conditions (velocity, depth, and Froude number), since the incline angle of the test chute can be readily adjusted. Future research could lead to refinement of a default relation that could be used for untested screens, verification of the screen-specific relations developed here for wider ranges of flow conditions, and characterization of screens utilizing specific wire types. Development of relations between the C_{cv} performance curve and other wire properties (e.g., edge radius, relief angle, etc.) may be possible.

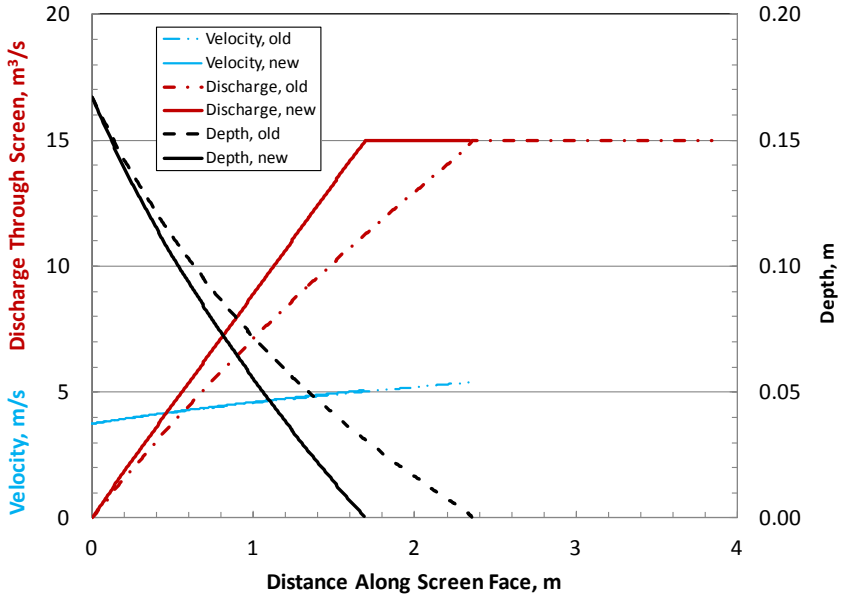

Figure 14. — Comparison of flow profiles for a hypothetical small hydro intake structure, using old (Wahl 2001) and new equations for computing C_{cv}.

REFERENCES

Wahl, Tony L., 2001. Hydraulic performance of Coanda-effect screens. *Journal of Hydraulic Engineering*, 127(6): 480-488.

Wahl, Tony L., 2003, *Design guidance for Coanda-effect screens*. U.S. Dept. of the Interior, Bureau of Reclamation, Research Report R-03-03. July 2003.

Wahl, Tony L., 2013. Coanda-Effect Screen Software. http://www.usbr.gov/pmts/hydraulics_lab/twahl/coanda/

THE AUTHOR

Tony L. Wahl is a Hydraulic Engineer with 23 years experience in the Bureau of Reclamation Hydraulics Laboratory at Denver, Colorado, working on an array of topics including flow measurement, fish screening, and dam breach modeling. Mr. Wahl is the developer of computer programs that are widely used for flume design, gate-flow calibration, Coanda-effect screen design, and ADV data analysis.